Supporting Information

Environment-friendly Mn-alloyed core/shell quantum dots for high-efficiency photoelectrochemical cells

Rui Wang[1], Xin Tong[1], Ali Imran Channa[1], Qiugui Zeng[1], Jiachen Sun[1], Cheng Liu[1], Xin Li[1], Jingyin Xu[1], Feng Lin[1], Gurpreet Singh Selopal[1,5], Federico Rosei[1,5], Yanning Zhang[1], Jiang Wu[1], Haiguang Zhao[2], Alberto Vomiero[3,4], Xuping Sun[1*] and Zhiming M. Wang[1*]*

1. Institute of Fundamental and Frontier Sciences, University of Electronic Science and Technology of China, Chengdu 610054, P. R. China.

2. State Key Laboratory of Bio-Fibers and Eco-Textiles & College of Physics, Qingdao University, No. 308 Ningxia Road, Qingdao 266071, P. R. China.

3. Division of Materials Science, Department of Engineering Sciences and Mathematics, Luleå University of Technology, SE-97187 Luleå, Sweden.

4. Department of Molecular Sciences and Nanosystems, Ca' Foscari University of Venice, Via Torino 155, 30170 Venezia Mestre, Italy.

5. Institut National de la Recherche Scientifique, Centre Énergie, Matériaux et Télécommunications, 1650 Boul. Lionel Boulet, Varennes, QC, J3X 1S2 Canada.

Corresponding authors: xin.tong@uestc.edu.cn, xpsun@uestc.edu.cn, zhmwang@uestc.edu.cn

Experimental section

Materials

Copper acetate ($Cu(Ac)_2$), indium acetate ($In(Ac)_3$), manganese acetate

($Mn(Ac)_2$), 1-dodecanethiol (DDT), oleylamine (OLA), oleic acid (OA), 1-octadecene (ODE), zinc acetate dihydrate ($Zn(Ac)_2 \cdot 2H_2O$), ethanol, isopropanol (IPA), toluene, sodium sulfide nonahydrate ($Na_2S \cdot 9H_2O$) and sodium sulfite (Na_2SO_3) were purchased from Sigma-Aldrich. Zirconium dioxide (ZrO_2) and sulfur were purchased from Aladdin. Ti-Nanoxide BL/SC was obtained from Solaronix. Titania paste containing ~20 nm nanoparticles in diameter (18 NR-T) and a mixture of active anatase particles (~20 nm) and larger anatase scatter particles (~450 nm) paste (18 NR-AO) were purchased from Dyesol (Queanbeyan, Australia). All chemicals and solvents were used without further treatments.

Synthesis of MnCIS/ZnS and CIS/ZnS core/shell QDs

MnCIS/ZnS QDs were synthesized by following the previous method with slight modifications [1]. Typically, 0.05 mmol $Cu(Ac)_2$, 0.05 mmol $In(Ac)_3$, 0.1 mmol $Mn(Ac)_2$, 0.2 mL of OA, and 5 mL of ODE were loaded into a three-neck flask and degassed at room temperature. The reaction system was evacuated for 30 min at 120 ℃, and then 0.2 mL of DDT was swiftly injected into the reaction solution. 0.3 mmol sulfur dissolved in 1.0 mL of OLA was quickly injected into the reaction solution at 180 ℃ and the growth of MnCIS QDs was held for 20 min before the coating of ZnS shell. After 20 min, 1 mL of 0.2 M $Zn(Ac)_2 \cdot 2H_2O$ dissolved in OA/ODE (with OA/ODE ratio of 1/4) was injected into the reaction flask and the temperature was increased to 230 ^oC for 30 min to grow the shell. The CIS/ZnS QDs were prepared using similar method but without the introduction of the $Mn(Ac)_2$ precursor. The as-synthesized QDs were precipitated by centrifugation with ethanol and toluene and

finally the centrifuged QDs were dispersed in toluene for future use.

PEC device preparation

Preparation of mesoporous TiO_2 and ZrO_2 film: fluorine-doped tin oxide (FTO) coated glass substrates were washed sequentially by acetone, ethanol and de-ionized water for 30 minutes in an ultrasonic machine and dried using N_2 gas. A compact pinhole-free TiO_2 layer was spin-coated on FTO glass substrates at 5000 r.p.m for 30s using a commercial Ti-Nanoxide BL/SC solution. The substrates were then annealed in air in a muffle furnace at 500 ℃ for 30 min.

Titania paste 18NR-AO was deposited on the TiO_2 compact layer by tape casting. The substrates were then dried in air for 13 min followed by heating on the plate at 120 ℃ for 6 min. The substrates were subsequently sintered in air in the furnace at 500 ℃ with a ramp rate of 5 ℃/min for 30 min. For preparation of ZrO_2 film, 1 g of ZrO_2 powder was blended with 5 mL IPA in a beaker under 12-hour magnetic stirring. The solvent was then removed by continuous magnetic stirring while connecting it to a pump until the volume of the mixture got reduced to half of starting volume. A single layer ZrO_2 film was deposited on FTO glass by tape casting, then annealed in a muffle furnace at 450 ℃ for 30 min.

Electrophoretic deposition (EPD) was employed to deposit QDs on the TiO_2 film. Two pieces of as-prepared TiO_2 FTO were vertically soaked in the QDs solution, kept at 1 cm distance. A direct current bias source of 100 V was applied for 60 min, then washed with toluene and dried in N_2 flow. The successive ionic layer adsorption and reaction (SILAR) method was used to deposit a ZnS layer on the as-prepared

QDs/TiO_2/FTO electrode to avoid photocorrosion. Typically, the QDs/TiO_2/FTO photoanode was immersed into a 0.1 M solution of $Zn(Ac)_2$ for 1 min then transferred into 0.1 M solution of Na_2S for 1 min. After each immersion, the photoanode was rinsed thoroughly with the corresponding solvents (methanol or methanol: DI-water), respectively, then dried by N_2.

Characterization

The morphology of the samples was analyzed by transmission electron microscopy (TEM) using a JEM-2100F microscope. X-ray diffraction (XRD) patterns were obtained using a D8 ADVANCE X-ray Diffractometer from Brucker equipped with Cu-K_α radiation. UV-visible-NIR absorption spectra were acquired with a UV-Vis spectrophotometer (Shimadzu UV-3101 PC). The morphology of the cross-section of the QDs/TiO_2/FTO samples was attained by using a FEI Inspect F50 scanning electron microscope (SEM) and the chemical composition mapping was obtained by EDS analysis. The chemical composition was studied with X-ray photoelectron spectroscopy (XPS), using a ULVAC-PHI Quantro SXM system. Photoluminescence (PL) spectra and PL lifetime of the QDs were acquired via a FLS920 fluorescence spectrometer equipped with an InGaAs NIR detector (Edinburgh Instrument, UK).

Photoelectrochemical measurements

The electrochemical measurements were performed on a Princeton 300A electrochemical workstation (PARSTAT 3000A-DX with 20 mV/s sweep rate), coupled with the three-electrode system: with as-fabricated photoanodes as working electrode, an Ag/AgCl (saturated with 3.0 M KCl) as the referenced electrode, and

platinum wire as the counter electrode. A class AAA solar simulator (ASN-EI, XES-50S1) was employed to irradiate the samples with one sun illumination (1 Sun = AM 1.5G, 100 $mW \cdot cm^{-2}$) for photocurrent–voltage (I–V) measurements. The distance between photoelectrode and solar simulator was maintained at ~12 cm as measured by a standard Si reference diode.

The Mott-Schottky curves were collected in the standard three-electrode system mentioned above. Electrochemical impedance spectroscopy (EIS) measurements were monitored at a fixed frequency of 1000 Hz with 10 mV amplitude of open circuit potentials, and then using the obtained capacitances for Mott-Schottky plots.

Calculation of theoretical value of hydrogen

$$H_2(mole) = \frac{Q}{2F} = \frac{I \times t}{2F} = \int_0^t \frac{I dt}{F}$$

Where Q, I and F are the quantity of the charge passed in time *t*, obtained photocurrent from the photoanode and Faraday's constant (96484.34 C/mol), respectively. In this case, the amount of the charge can be estimated by integrating the current (I) over time (t) because of the variable current voltage curve.

Table S1. XPS analysis of composition (atomic concentration) of MnCIS core QDs.

Element	Atom%
S	10.4
In	2.51
Cu	2.84
Mn	2.50

Table S2. Comparison of MnCIS/ZnS core/shell QDs based PEC devices with other similar QDs based PEC devices.

Type of QDs	Photocurrent Density (mA/cm^{-2})	Stability of Device	Faradaic Efficiency (FE)	Reference
CIS	~0.29			2
CIS	~1.92			3
CuZnSnS-AgS	~0.58			4
CIS	~4.1			5
CISeS/ZnS	~5.3	~77%		6
Zn-CISe/6CIS	~3.1	~69%		7
MnCIS/ZnS	~5.7	~73%	~74%	This work

Table S3. Lifetime components and percentage parameters of MnCIS/ZnS and CIS/ZnS QDs in toluene and coupled with various films/electrolyte (Ely).

	τ_1 (ns)	τ_2 (ns)	τ_3 (ns)	a_1	a_2	a_3
MnCIS/ZnS/Toluene	15.3	126.3	397.6	16%	60%	24%
MnCIS/ZnS/ZrO_2	5.1	16.1	84.5	22%	10%	68%
MnCIS/ZnS/ZrO_2-Ely	1.8	15.5	88.1	97%	1%	2%
MnCIS/ZnS/TiO_2	0.5	3.2	26.4	94%	3%	3%
CIS/ZnS/Toluene	14.1	53	183.2	10%	23%	67%
CIS/ZnS/ZrO_2	1.6	0.3	6.3	49%	7%	44%
CIS/ZnS/ZrO_2-Ely	1.7	1.1	8.4	36%	62%	2%
CIS/ZnS/TiO_2	1.2	0.9	9.5	3%	96%	1%

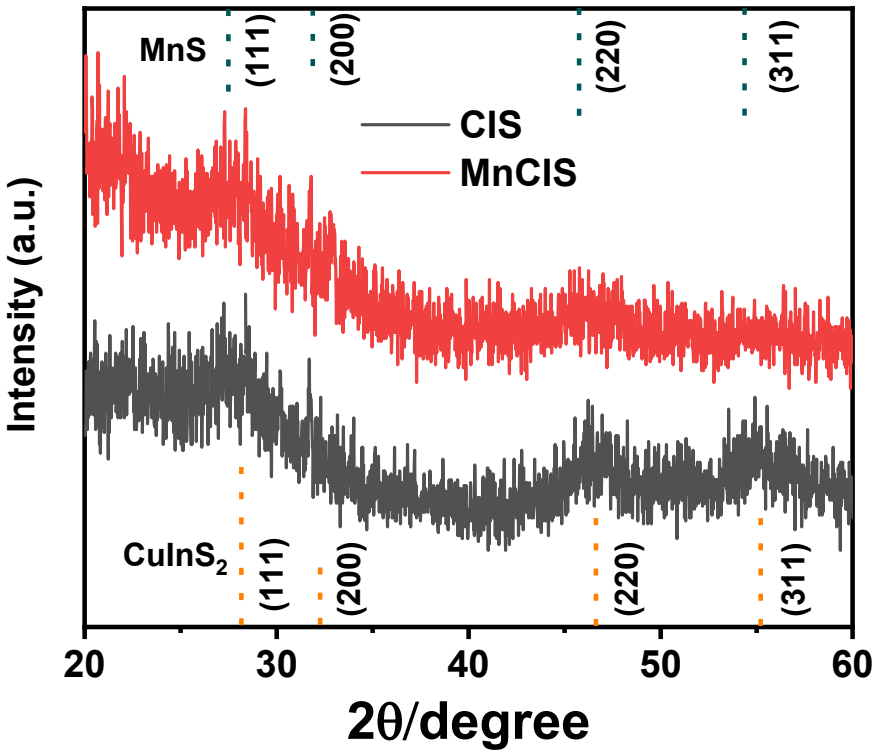

Figure S1. XRD patterns of MnCIS and CIS core QDs. All diffraction peaks of MnCIS QDs are located between the peaks of pure MnS and CIS, indicating the formation of alloyed MnCIS QDs.

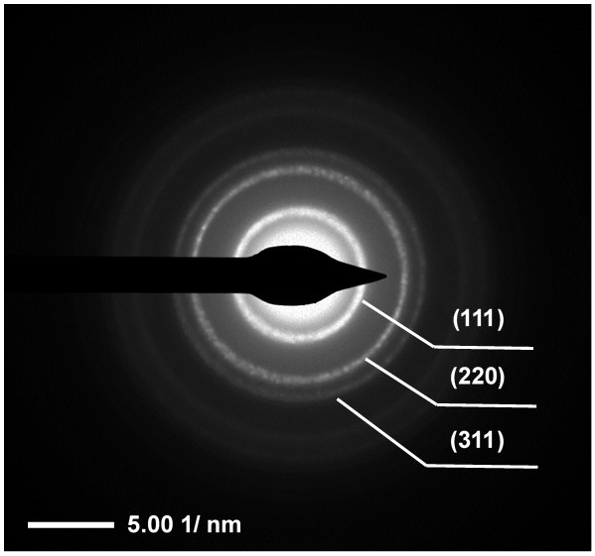

Figure S2. SAED pattern of MnCIS/ZnS core/shell QDs.

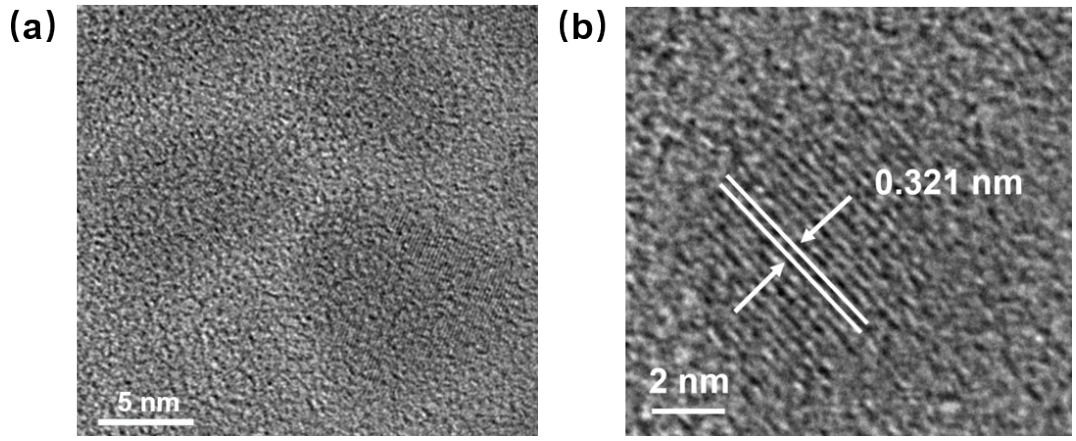

Figure S3. (a) TEM and (b) HRTEM images of MnCIS core QDs, showing lattice spacing of 0.324 nm that lies between the (111) plane of zincblende MnS (0.323 nm) and CIS (0.319 nm), demonstrating the successful formation of alloyed Mn alloyed CIS QDs.

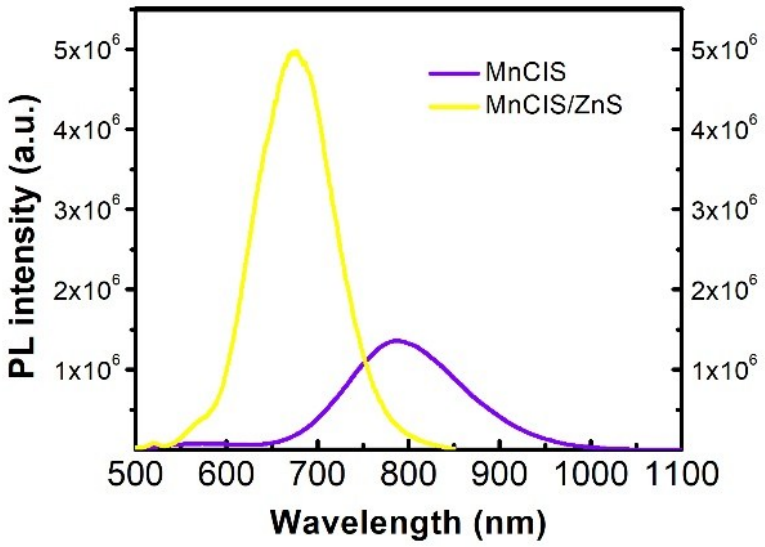

Figure S4. PL spectra of MnCIS core and MnCIS/ZnS core/shell QDs measured under identical concentration. The integrated PL intensity ratio between MnCIS/ZnS core/shell and MnCIS core QDs is calculated to be 2.4.

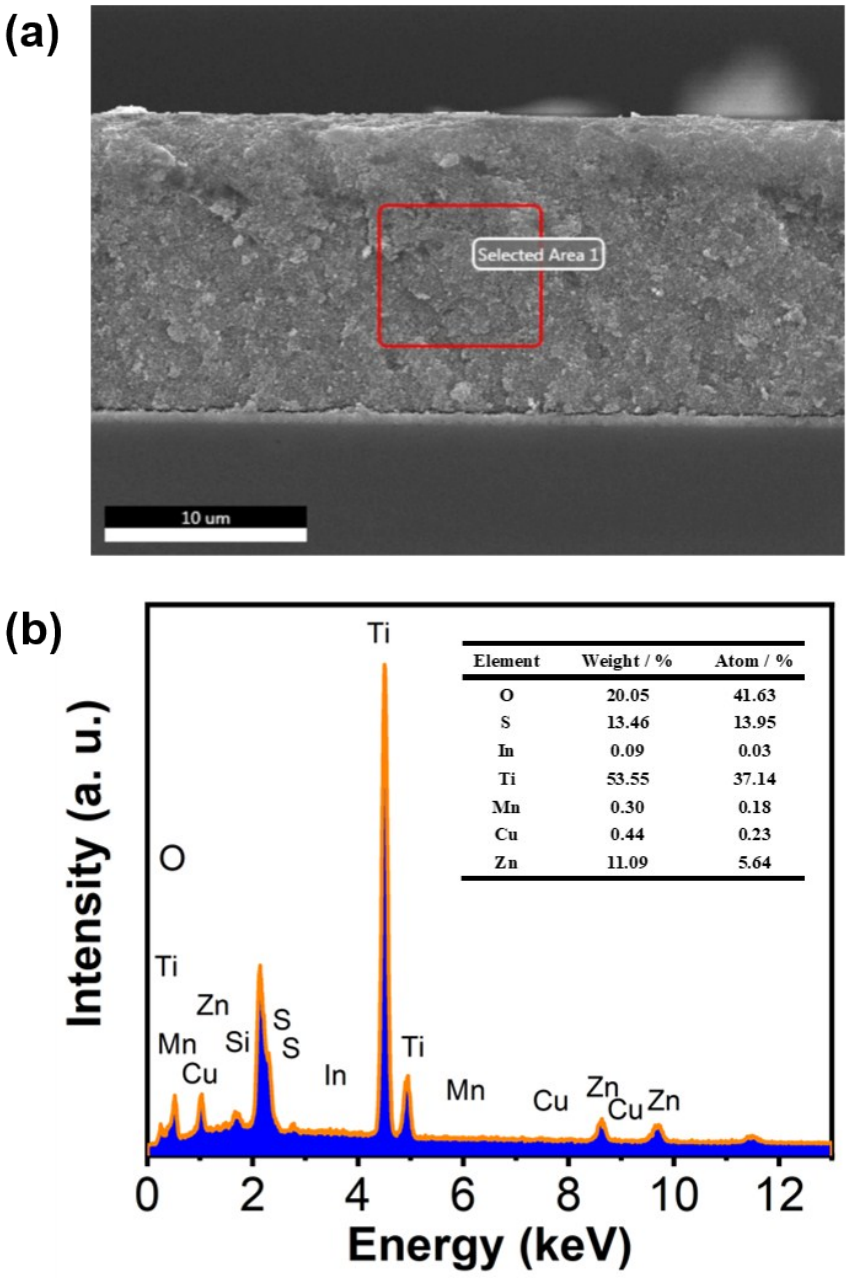

Figure S5. (a) Cross-sectional SEM image of MnCIS/ZnS/TiO_2 and corresponding (b) EDS spectrum recorded from a specified region (red solid line in (a)).

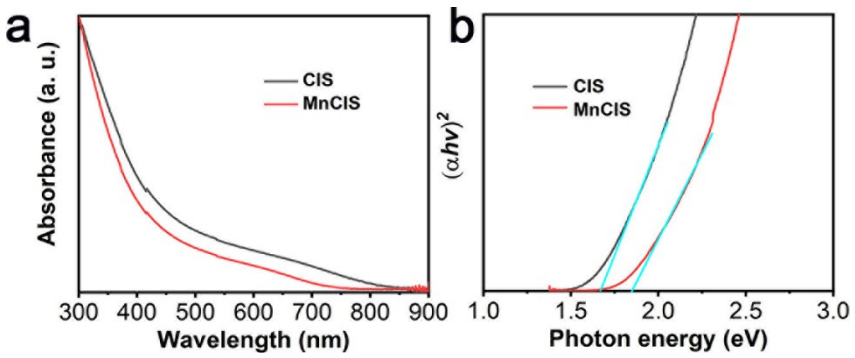

Figure S6. (a) Optical absorption spectra of CIS and MnCIS QDs in toluene. (b) Tauc plots $(\alpha h\upsilon)^2$ versus photon energy ($h\upsilon$) derived from (a).

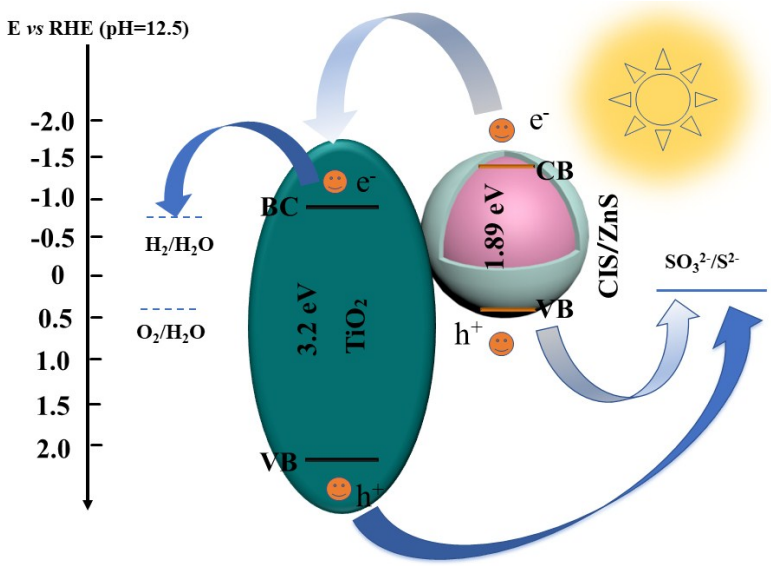

Figure S7. Band alignment and schematic diagram of CIS/ZnS QDs-sensitized photoanode.

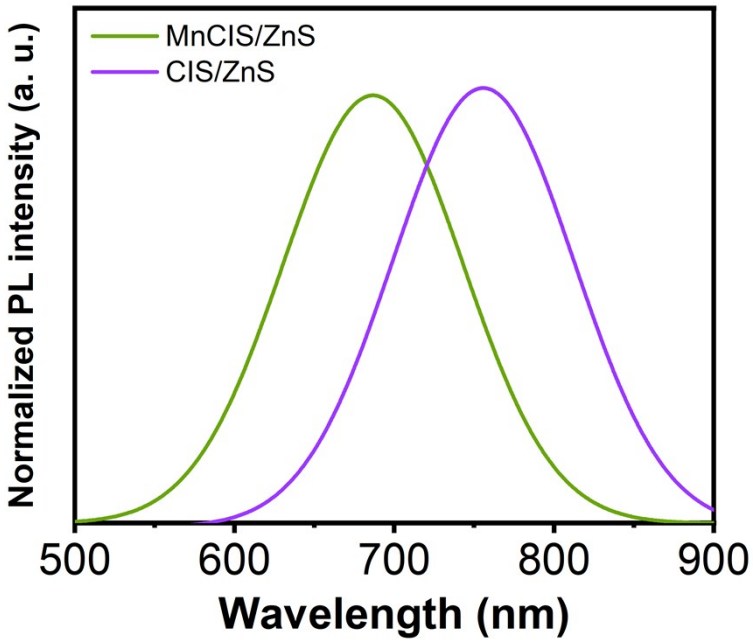

Figure S8. PL spectra of the MnCIS/ZnS and CIS/ZnS QDs in toluene.

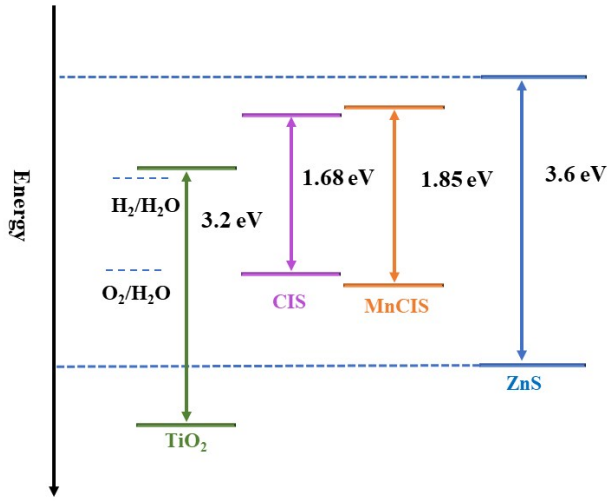

Figure S9. Relative band energy levels of MnCIS/ZnS and CIS/ZnS QDs with respect to TiO_2.

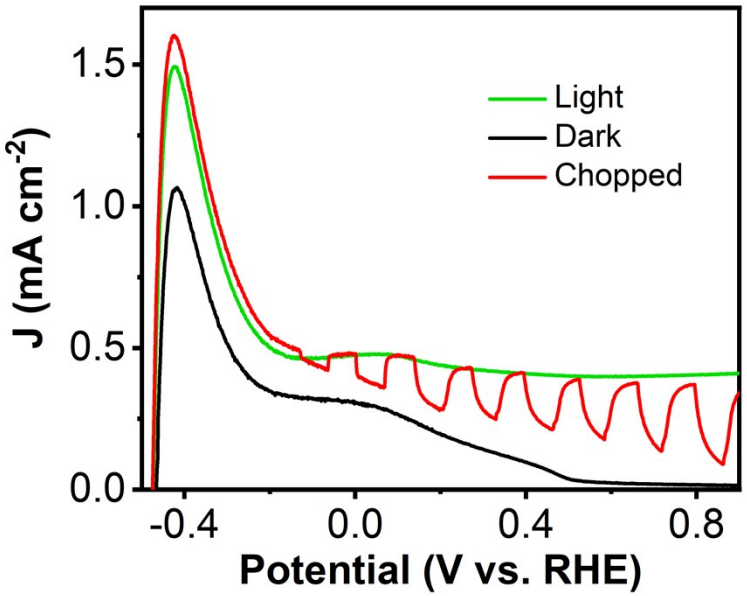

Figure S10. Linear sweep voltammetry of bare mesoporous TiO_2 based photoanode in dark, under continuous and chopped light illumination (AM 1.5 G, 100 mW/cm^2), showing photocurrent density of ~0.40 mA/cm^2.

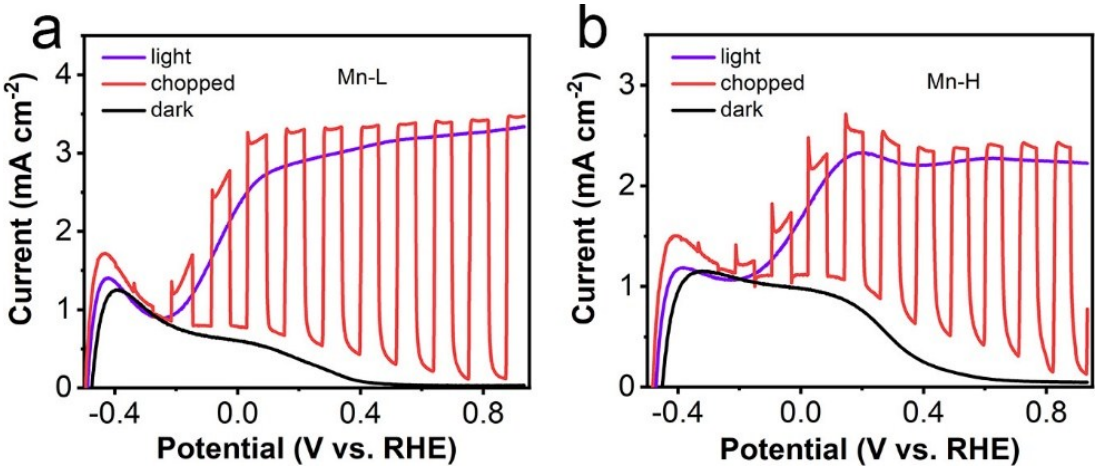

Figure S11. *J-V* curves for (a) the Mn-L and (b) Mn-H photoanodes in the dark, under continuous and chopped illumination (AM 1.5G, 100 mW/cm^2).

References

[1] Q. Liu, R. Deng, X. Ji, D. Pan, Nanotechnology 2012, 23, 255706.

[2] L. Wu, S. Y. Chen, F. J. Fan, T. T. Zhuang, C. M. Dai, S. H. Yu, J. Am. Chem.

Soc. 2016, 138, 5576.

[3] T.-L. Li, H. Teng, J. Mater. Chem. 2010, 20, 3656.

[4] X. Yu, J. Liu, A. Genç, M. Ibáñez, Z. Luo, A. Shavel, J. Arbiol, G. Zhang, Y. Zhang, A. Cabot, Langmuir 2015, 31, 10555.

[5] T.-L. Li, Y.-L. Lee, H. Teng, J. Mater. Chem. 2011, 21, 5089.

[6] X. Tong, Y. Zhou, L. Jin, K. Basu, R. Adhikari, G. S. Selopal, X. Tong, H. Zhao, S. Sun, A. Vomiero, Z. M. Wang, F. Rosei, Nano Energy 2017, 31, 441.

[7] X. Tong, X.-T. Kong, Y. Zhou, F. Navarro-Pardo, G. S. Selopal, S. Sun, A. O. Govorov, H. Zhao, Z. M. Wang, F. Rosei, Adv. Energy Mater. 2018, 8.